

APPLICATION FOR UNITED STATES LETTERS PATENT

FOR

**AMPLIFIER PRE-DISTORTION PROCESSING BASED ON COMPOSITE LOOK-UP TABLES**

Inventors: Robert E. Johnson  
Ruikang Yang

Prepared by: Mendelsohn & Associates, P.C.  
1515 Market Street, Suite 715  
Philadelphia, Pennsylvania 19102  
(215) 557-6657  
Customer No. 22186

\*

\*

\*

\*

\*

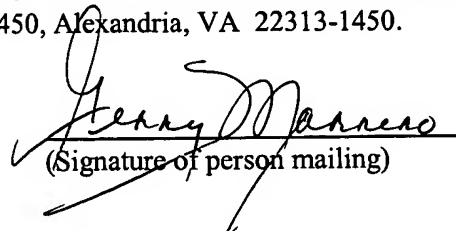
Certification Under 37 CFR 1.10

"Express Mail" Mailing Label No. EV140154294US

Date of Deposit 10/22/03

I hereby certify that this document is being deposited with the United States Postal Service's "Express Mail Post Office To Addressee" service under 37 CFR 1.10 on the date indicated above and is addressed to the Commissioner for Patents, P.O. Box 1450, Alexandria, VA 22313-1450.

Gerry Marrero  
(Name of person mailing)

  
(Signature of person mailing)

## AMPLIFIER PRE-DISTORTION PROCESSING BASED ON COMPOSITE LOOK-UP TABLES

### Field of the Invention

The present invention relates to signal processing, and, in particular, to techniques for linearizing  
5 amplifiers based on pre-compensation.

### Background of the Invention

Amplifiers, such as high-power amplifiers used in the base stations of wireless communication  
systems, typically exhibit non-linearity over their operating ranges. This non-linearity can result in noise  
10 that can corrupt or otherwise interfere with the communications. To address this problem, additional  
circuitry may be added to an amplifier in an attempt to linearize the effective amplifier response.  
Conventional techniques for linearizing amplifiers typically involve pre-compensation and/or feed-  
forward compensation.

In amplifier linearization based on pre-compensation, the input signal that is to be amplified is  
15 pre-distorted prior to being applied to the amplifier in order to adjust the input signal based on known  
non-linearities in the amplifier transfer function. In feed-forward compensation, an auxiliary signal is fed  
forward and combined with the output of the amplifier to adjust the output signal for non-linearities in  
the amplifier transfer function.

Fig. 1 shows a high-level block diagram of prior art amplifier system **100**, which is linearized  
20 using pre-compensation. In particular, a sample of an RF input signal  $x(t)$  is applied to envelope detector  
**102**, which generates a voltage representative of the instantaneous envelope power level of the input  
signal. This analog power signal  $p(t)$  is digitized by analog-to-digital converter (ADC) **104**. The  
resulting digital power signal  $p(n)$  is applied to pre-distorter **106**, which generates a pre-distorted signal  
in the form of digital pre-distortion component signals  $I(n)$  and  $Q(n)$ . These digital pre-distortion signals  
25  $I(n)$  and  $Q(n)$  are converted to analog pre-distortion signals  $I(t)$  and  $Q(t)$  by digital-to-analog converters  
(DACs) **108**. The analog pre-distortion signals  $I(t)$  and  $Q(t)$  are used by vector modulator **110** to  
modulate a delayed version of the RF input signal  $x(t)$  delayed by delay line **114** to generate a pre-  
distorted RF signal  $y(t)$  that is then input to amplifier **112**, which generates an amplified RF output signal  
 $z(t)$ . The purpose of RF delay line **114** is to compensate for the processing time of elements **102-108** to  
30 ensure that vector modulator **110** uses appropriately time-aligned pre-distortion signals  $I(t)$  and  $Q(t)$  to  
modulate the RF input signal  $x(t)$ . (Although Fig. 1 shows pre-distortion being applied to the input signal  
in the analog domain using a vector modulator, in alternative embodiments, pre-distortion can be applied  
to a baseband representation of the input signal in the digital domain.)

Delaying RF signals can be expensive (e.g., about \$1 for each nanosecond of delay). As such, one of the goals in implementing amplifier system **100** is to reduce the overall processing time of elements **102-108** to keep the delay required to be imparted by RF delay line **114** as small as possible. Moreover, the larger the delay line, the greater the attenuation of the RF signal. As such, gain is typically added to the amplifier to account for this attenuation, resulting in further cost and increased distortion.

### Brief Description of the Drawings

Aspects, features, and advantages of the present invention will become more fully apparent from the following detailed description, the appended claims, and the accompanying drawings in which like reference numerals identify similar or identical elements.

Fig. 1 shows a high-level block diagram of a prior art amplifier system that is linearized using pre-compensation;

Fig. 2 shows a block diagram of a pre-distorter that can be used to implement the pre-distorter of Fig. 1;

Fig. 3 shows a block diagram of an alternative pre-distorter that can be used to implement the pre-distorter of Fig. 1;

Fig. 4 shows a block diagram of another alternative pre-distorter that can be used to implement the pre-distorter of Fig. 1; and

Fig. 5 shows a block diagram of a RAM-based pre-distorter that can be used to implement the pre-distorter of Fig. 1.

### Detailed Description

Fig. 2 shows a block diagram of prior art pre-distorter **206**, which can be used to implement the pre-distorter of Fig. 1. In particular, Fig. 2 shows ADC **204** (similar to ADC **104** of Fig. 1) receiving an analog voltage signal  $p(t)$  generated by an envelope detector (similar to envelope detector **102** of Fig. 1) and generating a digital signal  $p(n)$  corresponding to that received voltage and representative of the instantaneous RF envelope power level. The digital power signal  $p(n)$  is applied to pre-distorter **206**, which generates two digital pre-distortion components  $I(n)$  and  $Q(n)$ , each of which is applied to a DAC **208** (similar to DACs **108** of Fig. 1) to generate analog pre-distortion signals  $I(t)$  and  $Q(t)$  that are applied to a vector modulator (similar to vector modulator **110** of Fig. 1) to generate a pre-distorted signal for amplification by an amplifier (similar to amplifier **112** of Fig. 1).

Pre-distorter **206** of Fig. 2 may be implemented in a field-programmable gate array (FPGA) or other suitable processor. As shown in Fig. 2, pre-distorter **206** has input delay module **216** (e.g., a flip-flop), which is an optional part of the FPGA's I/O circuitry. The envelope power signal from module

216 is applied in parallel to primary I look-up table (LUT) 218, differential I LUT 220, primary Q LUT 222, and differential Q LUT 224, each of which stores a different set of digital pre-distortion parameter values (i.e., correction coefficients) that are initially derived using off-line calibration procedures under different operating conditions. Primary LUTs 218 and 222 preferably store frequency-independent I and Q pre-distortion parameters (also referred to as “layer 1” parameters), respectively, while differential LUTs 220 and 224 preferably store frequency-dependent I and Q pre-distortion parameters (also referred to as “layer 2” parameters), respectively. The envelope power signal  $p(n)$  is used as an index to retrieve corresponding pre-distortion parameters from the LUTs.

Delay modules 226, 228, and 230, difference node 232, and summation node 234 are designed to generate a digital pre-distortion component  $I(n)$  according to Equation (1) as follows:

$$I(n) = I_{p1}(p(n)) + (I_{d1}(p(n+1)) - I_{d1}(p(n-1))) \quad (1)$$

where  $I_{p1}(p(n))$  is the primary I pre-distortion parameter from LUT 218 for the current power sample  $p(n)$ ,  $I_{d1}(p(n-1))$  is the differential I pre-distortion parameter from LUT 220 for the previous power sample  $p(n-1)$ , and  $I_{d1}(p(n+1))$  is the differential I pre-distortion parameter from LUT 220 for the next power sample  $p(n+1)$ .

Similarly, delay modules 236, 238, and 240, difference node 242, and summation node 244 are designed to generate a digital pre-distortion component  $Q(n)$  according to Equation (2) as follows:

$$Q(n) = Q_{p1}(p(n)) + (Q_{d1}(p(n+1)) - Q_{d1}(p(n-1))) \quad (2)$$

where  $Q_{p1}(p(n))$  is the primary Q pre-distortion parameter from LUT 222 for the current power sample,  $Q_{d1}(p(n-1))$  is the differential Q pre-distortion parameter from LUT 224 for the previous power sample, and  $Q_{d1}(p(n+1))$  is the differential Q pre-distortion parameter from LUT 224 for the next power sample.

The purpose of delay nodes 226-230 and 236-240 is to properly align the various pre-distortion parameters in time to implement the desired equations.

The resulting pre-distortion components  $I(n)$  and  $Q(n)$  are applied to output delay modules 246 and 248, which are optional parts of the FPGA's I/O circuitry, and converted to analog pre-distortion signals  $I(t)$  and  $Q(t)$  by DACs 208 for application to the vector modulator.

Due to the time delays caused by signal processing, the circuitry of Fig. 2 adds a delay between the ADC and the DACs. Implementing an RF delay line, such as RF delay line 114, to compensate for such delays can be prohibitively expensive.

Fig. 3 shows a block diagram of alternative pre-distorter 306, which can be used to implement the pre-distorter of Fig. 1 with a smaller delay. In particular, Fig. 3 shows ADC 304 receiving an analog voltage signal  $p(t)$  generated by an envelope detector and generating a digital signal  $p(n)$  corresponding to that received voltage and representative of the instantaneous RF envelope power level. The digital

power signal  $p(n)$  is applied to pre-distorter **306**, which generates two digital pre-distortion components  $I(n)$  and  $Q(n)$ , each of which is applied to a DAC **308** to generate analog pre-distortion signals  $I(t)$  and  $Q(t)$  that are applied to a vector modulator to generate a pre-distorted signal for application to an amplifier.

Like pre-distorter **206** of Fig. 2, pre-distorter **306** has input delay module **316** and two output delay modules **346** and **348**, which are optional parts of the FPGA's I/O circuitry. In addition, like pre-distorter **206**, pre-distorter **306** has primary and differential LUTs **318-324** that store (frequency-dependent and frequency-independent) pre-distortion parameter values.

Unlike pre-distorter **206**, which has circuitry that implements Equations (1) and (2), however, pre-distorter **306** has circuitry that implements Equations (3) and (4) as follows:

$$I(n) = I_{p2}(p(n)) + I_{d2}(p(n) - p(n-1)) \quad (3)$$

$$Q(n) = Q_{p2}(p(n)) + Q_{d2}(p(n) - p(n-1)) \quad (4)$$

where  $I_{p2}(p(n))$  is the primary I pre-distortion parameter from LUT **318** for the current power sample,  $I_{d2}(p(n) - p(n-1))$  is the differential I pre-distortion parameter from LUT **320** for the difference between the current power sample and the previous power sample,  $Q_{p2}(p(n))$  is the primary Q pre-distortion parameter from LUT **322** for the current power sample, and  $Q_{d2}(p(n) - p(n-1))$  is the differential Q pre-distortion parameter from LUT **324** for the difference between the current power sample and the previous power sample. Note that, while the pre-distortion parameter data stored in primary LUTs **318** and **322** will typically be identical to that stored in primary LUTs **218** and **222** of Fig. 2, differential LUTs **320** and **324** will store I and Q parameter data that differs from differential LUTs **220** and **224** of Fig. 2, since LUTs **320** and **324** are indexed using power differences.

Pre-distorter **306** has delay **328** and difference node **332**, which generate the difference between the current power sample  $p(n)$  and the previous power sample  $p(n-1)$ . This difference is applied to the I and Q differential LUTs **320** and **324**. Pre-distorter **306** also has summation nodes **334** and **344**, which sum the outputs of the two I LUTs and the outputs of the two Q LUTs, respectively.

Comparing Figs. 2 and 3, pre-distorter **306** is implemented using two fewer delay elements, with one fewer delay element in each of the I and Q processing paths. As a result, the overall processing time for pre-distorter **306** can be less than the overall processing time for pre-distorter **206** of Fig. 2, resulting in a less expensive RF delay line for the amplifier system. The shorter overall processing time can provide improved performance, e.g., for applications in which reducing signal latency is advantageous.

Although pre-distorter **306** of Fig. 3 has summation nodes **334** and **344**, an analogous pre-distorter can be implemented using difference nodes by storing data having opposite signs in the appropriate LUTs.

Fig. 4 shows a block diagram of another alternative pre-distorter **406**, which can be used to implement the pre-distorter of Fig. 1. In particular, Fig. 4 shows ADC **404** receiving an analog voltage signal  $p(t)$  generated by an envelope detector and generating a digital signal  $p(n)$  corresponding to that received voltage and representative of the instantaneous RF envelope power level. The digital power signal  $p(n)$  is applied to pre-distorter **406**, which generates two digital pre-distortion components  $I(n)$  and  $Q(n)$ , each of which is applied to a DAC **408** to generate analog pre-distortion signals  $I(t)$  and  $Q(t)$  that are applied to a vector modulator to generate a pre-distorted signal for application to an amplifier.

Like pre-distorter **206** of Fig. 2 and pre-distorter **306** of Fig. 2, pre-distorter **406** has input delay module **416** and two output delay modules **446** and **448**, which are optional parts of the FPGA's I/O circuitry. In addition, like pre-distorter **206** and pre-distorter **306**, pre-distorter **406** has primary and differential LUTs **418-424** that store pre-distortion parameter values.

Unlike pre-distorter **206**, which has circuitry that implements Equations (1) and (2), and pre-distorter **306**, which has circuitry that implements Equations (3) and (4), however, pre-distorter **406** has circuitry that implements Equations (5) and (6):

$$I(n) = I_{p3}(p(n)) - I_{d3}(p(n-1)) \quad (5)$$

$$Q(n) = Q_{p3}(p(n)) - Q_{d3}(p(n-1)) \quad (6)$$

where  $I_{p3}(p(n))$  is the primary I pre-distortion parameter from LUT **418** for the current power sample,  $I_{d3}(p(n-1))$  is the differential I pre-distortion parameter from LUT **420** for the previous power sample,  $Q_{p3}(p(n))$  is the primary Q pre-distortion parameter from LUT **422** for the current power sample, and  $Q_{d3}(p(n-1))$  is the differential Q pre-distortion parameter from LUT **424** for the previous power sample. As before, the pre-distortion parameter data stored in these LUTs may differ from the data stored in the LUTs of the other embodiments.

Pre-distorter **406** has delay **428** and difference nodes **432** and **442**, which generate the differences between the primary I and Q pre-distortion parameters for the current power sample  $p(n)$  and the differential I and Q pre-distortion parameters for the previous power sample  $p(n-1)$ , respectively.

Comparing Figs. 3 and 4, pre-distorter **306** is implemented using one difference node (**332**) and two summation nodes (**334** and **344**), while pre-distorter **406** is implemented using two difference nodes (**432** and **442**) and no summation nodes. In addition, to using one fewer node, pre-distorter **406** has one less difference/summation operation in each of the I and Q processing paths. As a result, the overall processing time for pre-distorter **406** can be less than the overall processing time for pre-distorter **306**, resulting in an even less expensive RF delay line for the amplifier system. As before, the shorter overall processing time can provide improved performance, e.g., for applications in which reducing signal latency is advantageous.

Although pre-distorter **406** of Fig. 4 has difference nodes **432** and **442**, an analogous pre-distorter can be implemented using summation nodes by storing data having opposite signs in the appropriate LUTs.

Equations (5) and (6) and the architecture of Fig. 4 enable a RAM-based implementation as opposed to the FPGA-based implementations of Figs. 2-4.

Fig. 5 shows a block diagram of a RAM-based pre-distorter **506**, which can be used to implement the pre-distorter of Fig. 1. In particular, Fig. 5 shows ADC **504**, which receives an analog voltage signal  $p(t)$  generated by an envelope detector and outputs two digital values, one (**550**) corresponding to current RF envelope power level  $p(n)$  and the other (**552**) corresponding to the previous RF envelope power level  $p(n-1)$ . In one implementation, ADC **504** is designed to output the current and previous samples at every ADC operating cycle. In addition, ADC **504** outputs a clock signal **554** that is applied to activate DACs **508**.

At the heart of pre-distorter **506** are two single-port asynchronous RAMs **556**, one for storing I pre-distortion parameters in a single, composite I LUT and one for storing Q pre-distortion parameters in a single, composite Q LUT. According to this implementation, each composite LUT receives a single combined index value, where half of the bits correspond to the current digital power level  $p(n)$  from ADC **504** and the remaining bits correspond to the previous digital power level  $p(n-1)$  from ADC **504**, where the two power levels are concatenated or appended together to form the combined index. In essence, each composite LUT maps all possible combinations of consecutive power levels to the corresponding pre-distortion parameters, thereby avoiding the need for any additional computational circuitry, such as that shown in Figs. 2-4. In particular, for  $m$ -bit current and previous power levels, RAM-based LUTs **556** map  $2^{2m}$  different combined indices to corresponding  $I(n)$  and  $Q(n)$  pre-distortion components.

These  $I(n)$  and  $Q(n)$  pre-distortion signals are applied to DACs **508** to generate analog pre-distortion signals  $I(t)$  and  $Q(t)$  that are applied to a vector modulator to generate a pre-distorted signal for application to an amplifier.

In addition, pre-distorter **506** has controller **558**, switches **560** and **562**, delay **564**, and inverter **566**, which enable RAMs **556** to be loaded with I and Q pre-distortion parameter values during initialization and possibly during intermittent dynamic LUT updating. In particular, to load RAMs **556**, controller **558** disables switches **560** and **562** to prevent the ADC outputs from reaching RAMs **556**. At the same time, controller **558** configures RAMs **556** to receive I and Q pre-distortion parameter values via data line **568**, while clock control line **570** disables DACs **508**.

Depending on the particular implementation, controller 558 may be a DSP, a CPLD, an FPGA, or any other suitable processing device. Switches 560 and 562 may be implemented using FET switches, and RAMs 556 may be implemented using two asynchronous RAMs.

The implementation of Fig. 5 is capable of a significant reduction in the total processing time of pre-distorter 506 and thus a significant reduction in the cost of implementing such an amplifier system.

In each of the implementations shown in Figs. 2-5, the DACs could be replaced with digital modulators.

The present invention may be implemented in the context of wireless signals transmitted from a base station to one or more mobile units of a wireless communication network. In theory, embodiments of the present invention could be implemented for wireless signals transmitted from a mobile unit to one or more base stations. The present invention can also be implemented in the context of other wireless and even wired communication networks to reduce spurious emissions.

Embodiments of the present invention may be implemented as circuit-based processes, including possible implementation on a single integrated circuit (such as an ASIC or an FPGA), a multi-chip module, a single card, or a multi-card circuit pack. As would be apparent to one skilled in the art, various functions of circuit elements may also be implemented as processing steps in a software program. Such software may be employed in, for example, a digital signal processor, micro-controller, or general-purpose computer.

It will be further understood that various changes in the details, materials, and arrangements of the parts which have been described and illustrated in order to explain the nature of this invention may be made by those skilled in the art without departing from the scope of the invention as expressed in the following claims.